Hybrid Beamforming in Sub-THz LoS MIMO Systems

Chaewon Yun[*], Kae won Choi[°]

ABSTRACT

In this study, we design a hybrid beamforming algorithm for sub-terahertz-band communications. We introduce a near-field propagation model for an indoor line-of-sight environment. A hybrid beamforming method for sparse arrays of subarray structures is proposed. Using MATLAB simulation results, we show that the proposed algorithm achieves high capacity.

Key Words : Hybrid Beamforming, Sub-THz communication

I. Introduction

Sub-terahertz (sub-THz) band communication is expected to become key technologies for next-generation cellular systems[1]. Its abundant spectral resources enable faster and larger data transmission. Furthermore, its short wavelength allows an extremely high MIMO gain to be achieved via the arrangement of several antennas in a small form factor, which compensates for severe free-space path loss. Hybrid beamforming is proposed to efficiently connect RF chains to many antennas.

Hybrid beamforming is typically achieved by separating channel estimation and precoding matrix computations. However, because channel estimation for each individual antenna element in hybrid beamforming is challenging, the actual mmWave or sub-THz hybrid beamforming scheme applies a scanning method based on a focused beam and received power measurement. As the number of propagation paths in high-frequency systems is limited, near-optimal performance can be achieved by combining a few beams with high-gain paths.

Previously, two main hybrid beamforming antenna structures were fully and partially connected. The authors[2] compared array-of-subarray (AoSA) structures with fully connected structures in terms of spectral and energy efficiency, and proposed AoSAs as a promising solution for high-frequency bands.

Conventional channel models are based on planar wavefront assumptions. However, owing to the short wavelength and large array aperture in the sub-THz band, receivers are likely to be in the near-field region[3]. Therefore, a MIMO channel should be modeled based on a spherical wavefront using the AoSA structure.

The remainder of this paper is organized as follows: In Section II, we describe the channel model and antenna structure. Section III describes the proposed hybrid beamforming algorithm based on a scanning method. Subsequently, numerical results are provided in Section IV. The conclusions are presented in Section V.

II. System Model

In this section, we introduce the spherical wave channel model for the sparse array of subarray (SAoSA) structure.

Consider the hybrid-beamforming AoSA structure shown in Fig. 1(a), where each subarray is connected to a dedicated RF chain. We focus specifically on the SAoSA antenna structure, where the subarray spacing is relatively large, as shown in Fig. 1(b).

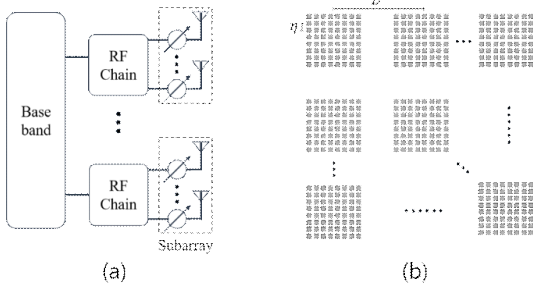First, we derived the channel between a single

Fig. 1. (a) Hybrid beamforming AoSA structure with RF chain; (b) SAoSA antenna structure

transmitting antenna element and receiver antenna element. This allow us to model the distance between antenna elements via line-of-sight (LoS) and non-line-of-sight (NLoS) paths. Subsequently, we extended the channel model to the SAoSA structure.

2.1 LOS Distance

We derived the LoS distance of the path between a single transmitting antenna element and a receiver antenna element. A local coordinate system (LCS) was adopted to represent the position and attitude of the antenna. Let the column vectors $\mathbf{c}^{Tx}$ and $\mathbf{c}^{Rx}$ denote the coordinates of the origins of the transmitter and receiver LCS, respectively. Let the column vectors $\mathbf{a}_l^{Tx}$ and $\mathbf{a}_m^{Rx}$ denote the coordinates of antenna l of the transmitter in the transmitter LCS and antenna m of the receiver in the receiver LCS, respectively. The rotation matrices of the transmitter and receiver LCS are denoted by $\mathbf{R}^{Tx}$ and $\mathbf{R}^{Rx}$, respectively. By performing a first-order approximation with the Taylor expansion $\sqrt{x^2 + y} \cong x + y/(2x)$, the LoS distance of the path between antenna l of the transmitter and antenna m of the receiver $d_{l,m}^{LoS}$ can be calculated as

$$
\begin{aligned}
d_{l,m}^{LoS} &= \left\| \left(\mathbf{c}^{Tx} + \mathbf{R}^{Tx}\mathbf{a}_l^{Tx}\right) \right.\\
&\quad \left. - \left(\mathbf{c}^{Rx} + \mathbf{R}^{Rx}\mathbf{a}_m^{Rx}\right) \right\| \\
&= \|\mathbf{r}\| + \frac{\mathbf{r}^T}{\|\mathbf{r}\|}\boldsymbol{\gamma}_{l,m} + \frac{\|\boldsymbol{\gamma}_{l,m}\|^2}{2\|\mathbf{r}\|} \qquad (1)\\
&= \|\mathbf{r}\| + \mathbf{q}^{Tx}\mathbf{a}_l^{Tx} + \mathbf{q}^{Rx}\mathbf{a}_m^{Rx} + \frac{\|\boldsymbol{\gamma}_{l,m}\|^2}{2\|\mathbf{r}\|},
\end{aligned}
$$

where $\|\mathbf{r}\| = \mathbf{c}^{Tx} - \mathbf{c}^{Rx}$ and $\boldsymbol{\gamma}_{l,m} = \mathbf{R}^{Tx}\mathbf{a}_l^{Tx} - \mathbf{R}^{Rx}\mathbf{a}_m^{Rx}$. Here, $\mathbf{q}^{Tx} = \frac{\mathbf{r}^T}{\|\mathbf{r}\|}\mathbf{R}^{Tx}$ and $\mathbf{q}^{Rx} = -\frac{\mathbf{r}^T}{\|\mathbf{r}\|}\mathbf{R}^{Rx}$ represent the incident directions at the transmitter and receiver of the LoS path, respectively.

2.2 NLOS Distance

The NLOS path distance can be derived by unfolding the path. The coordinate and rotation matrix of the receiver angle of arrival of path p are changed to $\mathbf{c}^{Rx(p)}$ and $\mathbf{R}^{Rx(p)}$, respectively. The NLoS distance of path p between antenna l of the transmitter and antenna m of the receiver is denoted by $d_{l,m}^{(p)}$.

Subsequently, we have

$$
\begin{aligned}
d_{l,m}^{(p)} &= \left\|\mathbf{r}^{(p)}\right\| + \frac{(\mathbf{r}^{(p)})^T}{\|\mathbf{r}^{(p)}\|}\boldsymbol{\gamma}_{l,m}^{(p)} + \frac{\left\|\boldsymbol{\gamma}_{l,m}^{(p)}\right\|^2}{2\|\mathbf{r}^{(p)}\|}\\
&= \left\|\mathbf{r}^{(p)}\right\| + \mathbf{q}^{Tx(p)}\mathbf{a}_l^{Tx} + \mathbf{q}^{Rx(p)}\mathbf{a}_m^{Rx} \qquad (2)\\
&\quad + \frac{\left\|\boldsymbol{\gamma}_{l,m}^{(p)}\right\|^2}{2\|\mathbf{r}^{(p)}\|},
\end{aligned}
$$

where $\mathbf{r}^{(p)} = \mathbf{c}^{Tx} - \mathbf{c}^{Rx(p)}$ and $\boldsymbol{\gamma}_{l,m}^{(p)} = \mathbf{R}^{Tx}\mathbf{a}_l^{Tx} - \mathbf{R}^{Rx(p)}\mathbf{a}_m^{Rx}$. Here, $\mathbf{q}^{Tx(p)} = \left((\mathbf{r}^{(p)})^T/\|\mathbf{r}^{(p)}\|\right)\mathbf{R}^{Tx}$ and $\mathbf{q}^{Rx(p)} = -\left((\mathbf{r}^{(p)})^T/\|\mathbf{r}^{(p)}\|\right)\mathbf{R}^{Rx(p)}$ represent the incident directions at the transmitter and receiver of path p, respectively.

2.3 Multipath Channel Model

We assume that the LoS path is the 0th path, i.e., $\mathbf{r}^{(0)} = \mathbf{r}$, $\boldsymbol{\gamma}_{l,m}^{(0)} = \boldsymbol{\gamma}_{l,m}$, $\mathbf{q}^{Tx(0)} = \mathbf{q}^{Tx}$, and $\mathbf{q}^{Rx(0)} = \mathbf{q}^{Rx}$.

Therefore, the channel is expressed as

$$
h_{(l,m),(i,j)}^{(p)} = \sum_{p=0}^{P} \frac{\alpha^{(p)}}{\|\mathbf{r}^{(p)}\|} \exp(-jk d_{(l,m)}^{(p)}), \qquad (3)
$$

where $\alpha^{(p)}$ is the path coefficient, which depends on the antenna gain, polarization, and transmittance/reflectance on path p; and k is the wave number.

2.4 SAoSA

In the SAoSA structure, N_{TS} transmit subarrays and N_{RS} receive subarrays are connected to dedicated N_A antenna elements. To extend the SAoSA structure, let the column vectors a_l^{Tx} and a_m^{Rx} denote the coordinates of subarray l of the transmitter in the transmitter LCS and those of subarray m of the receiver in the receiver LCS, respectively. Additionally, let column vectors $\delta_{l,i}^{Tx}$ and $\delta_{m,j}^{Rx}$ denote the displacement of antenna i of subarray l of the transmitter in the transmitter LCS and that of antenna j of subarray m of the receiver in the receiver LCS. Therefore, the distance of path p between antenna i of transmit subarray l and antenna j of receive subarray m is expressed as

$$
\begin{aligned}
d_{(l,m),(i,j)}^{(p)} &= \left\| \mathbf{r}^{(p)} \right\| + \mathbf{q}^{Tx(p)} a_l^{Tx} + \mathbf{q}^{Rx(p)} a_m^{Rx} \\
&+ \frac{\left\| \gamma_{l,m}^{(p)} \right\|^2}{2 \left\| \mathbf{r}^{(p)} \right\|} + \zeta_{l,m}^{Tx(p)} \delta_{l,i}^{Tx} + \zeta_{l,m}^{Rx(p)} \delta_{m,j}^{Rx},
\end{aligned}
\tag{4}
$$

where $\zeta_{l,m}^{Tx(p)}$ and $\zeta_{l,m}^{Rx(p)}$ are defined as

$$
\zeta_{l,m}^{Tx(p)} = \frac{\left(r^{(p)} + \gamma_{l,m}^{(p)}\right)^T}{\|r^{(p)}\|} R^{Tx}
\tag{5}
$$

and

$$
\zeta_{l,m}^{Rx(p)} = - \frac{\left(r^{(p)} + \gamma_{l,m}^{(p)}\right)^T}{\|r^{(p)}\|} R^{Rx(p)}
\tag{6}
$$

Consider a planar subarray with $N \times N$ antenna elements. We define $H_{l,m}$ as the channel matrix from the transmit array l to the receive subarray m. Therefore,

$$
\mathbf{H}_{l,m} = \sum_{p=0}^{P} H_{l,m}^{(p)}
\tag{7}
$$

Here,

$$
\mathbf{H}_{l,m}^{(p)} = \beta_{l,m}^{(p)} \left(h_{x,l,m}^{Rx(p)} \otimes h_{y,l,m}^{Rx(p)} \right) (h_{x,l,m}^{Tx(p)} \otimes h_{y,l,m}^{Tx(p)})^T,
\tag{8}
$$

where $\otimes$ denotes the Kronecker product. Furthermore,

$$
\beta_{l,m}^{(p)} = \frac{\alpha^{(p)}}{\|r^{(p)}\|} exp \left(-jk \left(\left\| r^{(p)} \right\| + q^{Tx(p)} a_l^{Tx} + q^{Rx(p)} a_m^{Rx} + \frac{\| \gamma_{l,m}^{(p)} \|^2}{2\|r^{(p)}\|} \right) \right)
\tag{9}
$$

and

$$
\begin{aligned}
\mathbf{h}_{x,l,m}^{Tx(p)} &= \\
&\left(exp\left(-jk\zeta_{x,l,m}^{Tx(p)} \eta \kappa_1^N \right), \dots, exp\left(-jk\zeta_{x,l,m}^{Tx(p)} \eta \kappa_N^N \right) \right)^T,
\end{aligned}
\tag{10}
$$

$$
\begin{aligned}
\mathbf{h}_{y,l,m}^{Tx(p)} &= \\
&\left(exp\left(-jk\zeta_{y,l,m}^{Tx(p)} \eta \kappa_1^N \right), \dots, exp\left(-jk\zeta_{y,l,m}^{Tx(p)} \eta \kappa_N^N \right) \right)^T,
\end{aligned}
\tag{11}
$$

$$
\begin{aligned}
\mathbf{h}_{x,l,m}^{Rx(p)} &= \\
&\left(exp\left(-jk\zeta_{x,l,m}^{Rx(p)} \eta \kappa_1^N \right), \dots, exp\left(-jk\zeta_{x,l,m}^{Rx(p)} \eta \kappa_N^N \right) \right)^T,
\end{aligned}
\tag{12}
$$

$$
\begin{aligned}
\mathbf{h}_{y,l,m}^{Rx(p)} &= \\
&\left(exp\left(-jk\zeta_{y,l,m}^{Rx(p)} \eta \kappa_1^N \right), \dots, exp\left(-jk\zeta_{y,l,m}^{Rx(p)} \eta \kappa_N^N \right) \right)^T,
\end{aligned}
\tag{13}
$$

$$
\kappa_N^N = (n-1) - (N-1)/2
\tag{14}
$$

III. Hybrid Beamforming Design

3.1 Beam Scanning and Combining

By controlling phase shifters, a beam can be formed and steered in the desired direction. Next, we consider the infinite resolution of phase shifters. If the beam is directed toward $v = (v_x, v_y, v_z)^T$, which is the beam direction of a subarray such that $\|v\| = 1$, then the weight vector is expressed as

$$
w(\mathbf{v}) = \mathbf{w}_x(v) \otimes \mathbf{w}_y(v)
\tag{15}
$$

$$
\begin{aligned}
\mathbf{w}_x(v) &= (exp(jkv_x \eta \kappa_1^N), \dots, exp(jkv_x \eta \kappa_N^N))^T
\end{aligned}
\tag{16}
$$

$$\mathbf{w}_x(v) = (\exp(jkv_y\eta\kappa_1^N), \dots, \exp(jkv_y\eta\kappa_N^N))^T \quad (17)$$

To steer the beam in strong directions, we scanned over the direction grid and selected the best N_B directions for each subarray. One possible codebook for scanning is $v_x = \sqrt{2}\kappa_i^N/(N-1)$ and $v_y = \sqrt{2}\kappa_j^N/(N-1)$ for $i = 1, \dots, N$ and $j = 1, \dots, N$. In this case, $N_B = N^2$.

Next, we present a signal model for transmitting N_L layers of data when the scanned beams are combined. Let $x \in C^{N_L \times 1}$ denote the data symbols and $P \in C^{N_{TS} \times N_L}$ denote the precoding matrix in the baseband. Let $W_l^{Tx} = (w_{l,1}^{Tx}, \dots, w_{l,N_B}^{Tx}) \in C^{N_A \times N_B}$ denote the candidate beam matrix at transmit subarray l, of which each column vector is the weight vector for the selected beam directions, and $\alpha_l^{Tx} \in C^{N_{TB} \times 1}$ denote the beam combining weight for the column vectors of W_l^{Tx}. Therefore, the beam matrix for the transmitting subarray l can be expressed as $s_l^{Tx} = W_l^{Tx}\alpha_l^{Tx}$. For the entire transmitter system, we define the candidate beam matrix for transmitter $U_{Tx} \in C^{N_{TS}N_A \times N_{TS}N_B}$ as a block diagonal matrix such that $U_{Tx} = diag(\{W_l^{Tx}\}_{l=1,\dots,N_{TS}})$, the beam combining weight matrix for transmitter $A_{Tx} \in C^{N_{TS}N_B \times N_{TS}}$ as a block diagonal matrix such that $A_{Tx} = diag(\{\alpha_l^{Tx}\}_{l=1,\dots,N_{TS}})$, and the beam matrix for transmitter $S_{Tx} = U_{Tx}A_{Tx} \in C^{N_{TS}N_A \times N_{TS}}$ as a block diagonal matrix such that $S_{Tx} = diag(\{s_l^{Tx}\}_{l=1,\dots,N_{TS}}$. Similarly, the beam combining weight matrix for the receiver, the candidate beam matrix for the receiver, and the beam matrix for the receiver are denoted as $A_{Rx} \in C^{N_{RS}N_B \times N_{RS}}$, $U_{Rx} \in C^{N_{RS}N_A \times N_{TS}N_B}$, and $S_{Rx} = U_{Rx}A_{Rx} \in C^{N_{RS}N_A \times N_{RS}}$, respectively; they are block diagonal matrices such that $A_{Rx} = diag(\{\alpha_m^{Rx}\}_{m=1,\dots,N_{RS}})$, $U_{Rx} = diag(\{W_m^{Tx}\}_{m=1,\dots,N_{RS}})$ with $W_m^{Rx} = (w(v_{m,1}^{Rx}), \dots, w(v_{m,N_B}^{Rx}))$ and $S_{Rx} = diag(\{s_l^{Rx}\}_{l=1,\dots,N_{RS}})$ with $s_l^{Rx} = W_l^{Rx}\alpha_l^{Rx}$. Furthermore, we define $C \in C^{N_{RS} \times N_L}$ as a combination matrix. The channel gain matrix from the transmitter to the receiver $H \in C^{N_{RS}N_A \times N_{TS}N_A}$ is a block matrix such that

$$H = \begin{pmatrix} H_{1,1} & H_{2,1} & \cdots & H_{N_{TS},1} \\ H_{1,2} & H_{2,2} & \cdots & H_{N_{TS},2} \\ \vdots & \vdots & \ddots & \vdots \\ H_{1,N_{RS}} & H_{2,N_{RS}} & \cdots & H_{N_{TS},N_{RS}} \end{pmatrix}$$

The received data symbol, denoted by $y \in C^{N_L \times 1}$, is expressed as

$$\begin{aligned} y &= \mathbf{C}^T S_{Rx}^T (HS_{Tx}Px + n) \\ &= \mathbf{C}^T A_{Rx}^T U_{Rx}^T (HU_{Tx}A_{Tx}Px + n), \end{aligned} \quad (18)$$

where $n \in C^{N_{RS}N_A \times 1}$ denotes the noise vector. This is a generalization of a typical hybrid beamforming model. If all the subarrays have the same position and attitude, then the model returns to a fully connected hybrid beamforming model.

3.2 Proposed Hybrid Beamforming Algorithm

We aim to design A_{Tx}, A_{Rx}, P, and C to maximize capacity. After selecting A_{Tx} and A_{Rx} such that the multiple beams are well focused, P and C can be calculated using SVD.

The received signal can be rewritten as

$$\begin{aligned} y &= \mathbf{Q}_{Rx}^T U_{Rx}^T \mathbf{H} U_{Tx} Q_{Tx}\mathbf{x} + \bar{\mathbf{n}} \\ &= \mathbf{Q}_{Rx}^T \bar{H} Q_{Tx}\mathbf{x} + \bar{\mathbf{n}}, \end{aligned} \quad (19)$$

where $Q_{Tx} \in C^{N_{TS}N_B \times N_L}$ and $Q_{Rx} \in C^{N_{RS}N_B \times N_L}$ are defined as $Q_{Tx} = A_{Tx}P$ and $Q_{Rx} = A_{Rx}C$, respectively; and $\bar{n} = C^T A_{Rx}^T U_{Rx}^T n$. Here, for the effective channel H, we define the SVD to be $\bar{H} = \Omega\Lambda\Phi^H$, where Ω and Φ are unitary matrices and Λ is a diagonal matrix of singular values organized in the descending order. The capacity is maximized if we approximate Q_{Tx} and Q_{Rx} as the first N_L columns of Ω^* and Φ, respectively. By vertically slicing Q_{Tx} and Q_{Rx} into N_{TS} and N_{RS}, respectively, we have rank-1 matrices $\{Q_{Tx,l}\}_{l=1,\dots,N_{TS}}$ and $\{Q_{Rx,m}\}_{m=1,\dots,N_{RS}}$, respectively, as A_{Tx} and A_{Rx} are block diagonal matrices. Therefore, we applied a low-rank approximation to obtain A_{Tx} and A_{Rx}. After considering the first N_L

columns of Ω^* and Φ and vertically slicing them into N_{RS} and N_{TS}, respectively, we define each matrix as $\omega_m \in C^{N_B \times N_L}$ for $m = 1, \ldots, N_{RS}$ and $\phi_l \in C^{N_B \times N_L}$ for $l = 1, \ldots, N_{TS}$. Using the SVDs of ϕ_l and ω_m, each α_l^{Tx} and α_m^{Rx} is set as the left-singular vector that corresponds to the highest singular value.

We define the new effective channel $\widetilde{H}$ as $\widetilde{H} = A_{Rx}^T U_{Rx}^T H U_{Tx} A_{Tx}$. Subsequently, we define the SVD of the effective channel matrix as

$$\widetilde{\mathbf{H}} = \widetilde{\mathbf{U}} \widetilde{\Sigma} \widetilde{V}^H, \tag{20}$$

where $\widetilde{U}$ and $\widetilde{V}$ are unitary matrices and $\widetilde{\Sigma}$ is a diagonal matrix with singular values on the diagonal.

Next, considering the transmit power p, the optimal digital precoder and combiner can be expressed as

$$P = \frac{\widetilde{V}}{\|\widetilde{V}\|_F} \sqrt{p} \tag{21}$$

$$C = \widetilde{U}^H \tag{22}$$

Ⅳ. Numerical Results

In this section, we present the numerical results to demonstrate the performance of the proposed hybrid beamforming algorithm.

We designed a ray tracing simulator to model indoor scenarios at a carrier frequency of 160 GHz. Fig. 2 shows the simulation scenarios. The transmitter and receiver faced each other in the presence of a clear LoS path. A uniform rectangular array was used for each subarray. At the transmitter and receiver, $N_{TS} = N_{RS} = 4$ subarrays were used, respectively, with element spacing η set as one-half the wavelength. The subarrays were placed on a two-dimensional grid and $N_L = 4$ layers were transmitted. The transmit power was 1 mW and the noise power was set as -70 dBm.

Fig. 3. shows the average spectral efficiency (SE) for the 16×16 and 32×32 element MIMO for
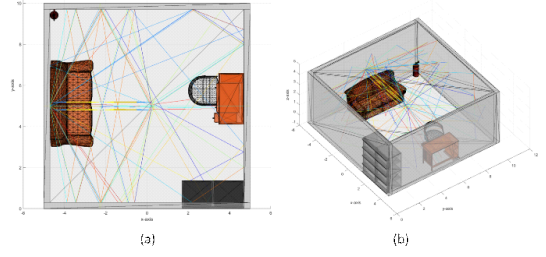

Fig. 2. Ray tracing Simulation Scenario (a) Top view; (b) side view
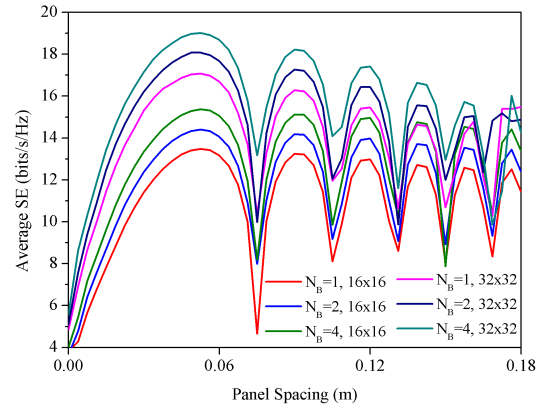

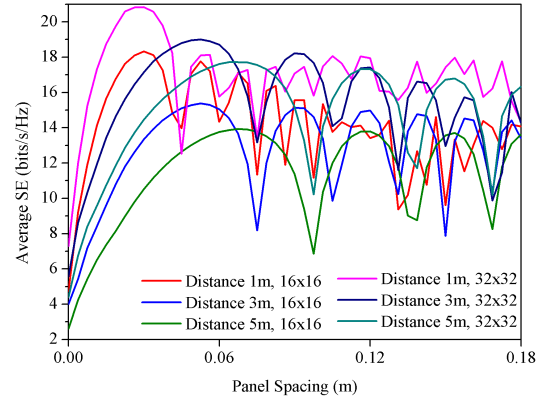Fig. 3. Average SE vs. panel spacing for different numbers of candidate beams

Fig. 4. Average SE vs. panel spacing for different LoS distances

different numbers of candidate beams when the subarray spacing between the arrays was varied. The lengths of the antenna arrays were 0.03 and 0.06 m for the 16×16 and 32×32 element arrays, respectively, and the LoS distance was 3 m. We observed that using more beams yielded better performance. In addition, because of interference,

when the arrays were placed closely together, the average SE increased with the panel spacing.

Fig. 4 shows a comparison of the performance of the algorithm with different LoS distances between the transmitter and receiver when $N_B = 4$. The result shows that a higher SE was achieved when a shorter distance and more elements were implemented.

Ⅴ. Conclusion

In this study, we proposed a hybrid beamforming algorithm for sub-THz systems. We developed a sub-THz channel model based on spherical wave propagation. Beam scanning and combined methods for the SAoSA antenna structure were introduced. MATLAB simulation results showed that the proposed algorithm achieved high capacity.

References

[1] T. S. Rappaport, et al., "Wireless communications and applications above 100 GHz: Opportunities and challenges for 6G and beyond," in *IEEE Access*, vol. 7, pp. 78729-78757, Jul. 2019.

[2] C. Lin and G. Y. L. Li, "Terahertz communications: An array-of-subarrays solution," in *IEEE Commun. Mag.*, vol. 54, no. 12, pp. 124-131, Dec. 2016.

[3] H. Sarieddeen, M. -S. Alouini, and T. Y. Al-Naffouri, "An overview of signal processing techniques for terahertz communications," in *Proc. IEEE*, vol. 109, no. 10, pp. 1628-1665, Oct. 2021. (https://doi:10.1109/JPROC.2021.3100811)